Membrane topological analysis of the proton-coupled folate transporter (PCFT-SLC46A1) by the substituted cysteine accessibility method[†]

Rongbao Zhao, **Ersin Selcuk Unal**, **Daniel Sanghoon Shin**, and **I. David Goldman**[*]
Departments of Medicine and Molecular Pharmacology, Albert Einstein College of Medicine, 1300 Morris Park Avenue, Bronx, NY, 10461 USA

Abstract

The proton-coupled folate transporter (PCFT) mediates intestinal folate absorption. Loss-of-function mutations in this gene are the molecular basis for the autosomal recessive disorder, hereditary folate malabsorption. In this study, the substituted cysteine accessibility method was utilized to localize extra- or intra-cellular loops connecting predicted PCFT transmembrane domains. Cysteine-less PCFT was generated by replacement of all seven cysteine residues with serine, and was shown to be functional, following which cysteine residues were introduced into predicted loops. HeLa cells, transiently transfected with these PCFT mutants, were then labeled with an impermeant, cysteine-specific biotinylation reagent (MTSEA-biotin) with or without permeabilization of cells. The biotinylated proteins were precipitated by streptavidin beads and assessed by Western blotting analysis. The biotinylation of PCFT was further confirmed by blocking cysteine residues with impermeant 2-sulfonatoethyl methanethiosulfonate. Two extracellular cysteine residues (66, 298) present in WT-PCFT were not biotinylated; however, in the absence of either one, biotinylation occurred. Likewise, biotinylation occurred after treatment with β-mercaptoethanol. Taken together, these analyses establish a PCFT secondary structure of twelve transmembrane domains with the N- and C- termini directed to the cytoplasm. The data indicate further that there is a disulfide bridge, which is not required for function, between the native C66 and C298 residues in the first and fourth transmembrane domains, respectively.

The proton-coupled folate transporter (PCFT; SLC46A1; NP_54200) was recently cloned and its critical role in intestinal absorption of folate vitamins established by this laboratory with the demonstration of loss-of-function mutations in the *pcft* gene in six unrelated families with the autosomal recessive disorder, hereditary folate malabsorption (HFM) (1,2). Since then, four additional subjects with the clinical diagnosis of HFM were shown to have mutations in this gene (3–6). PCFT also plays a critical role in transport of folates into the central nervous system since patients with HFM have very low folate levels in the cerebrospinal fluid (7,8) (GeneReviews, http://www.ncbi.nlm.nih.gov/bookshelf/br.fcgi?book=gene&part=folate-mal). PCFT mediated folate transport is electrogenic, optimal at low pH, and is accompanied by intracellular acidification (1,9–12).

[*]Corresponding author: I David Goldman, Departments of Medicine and Molecular Pharmacology, Albert Einstein College of Medicine, 1300 Morris Park Ave, Bronx, NY 10461, Tel: 718-430-2302, Fax: 718-430-8550, igoldman@aecom.yu.edu.

PCFT mediates antifolate absorption within the acidic microenvironment of the proximal small intestine. This is a particularly important route of administration for methotrexate in the treatment of autoimmune disorders, such as rheumatoid arthritis (13,14). PCFT plays an important role in pemetrexed transport into tumor cells (11); this is a novel antifolate approved for the treatment of pleural mesothelioma and non-small cell lung cancer (15–19). PCFT has a very high affinity for pemetrexed at the transporter's optimal low pH and retains a much higher affinity for this drug than other antifolates even at neutral pH, in the absence of a pH gradient, driven by the transmembrane voltage gradient (1,11). Hence, in the absence of the reduced folate carrier (SLC19A1), the major facilitative folate transporter that functions optimally at pH 7.4, pemetrexed transport is substantially preserved while transport of other antifolates, such as methotrexe, is impaired. This results in retention of pemetrexed activity even when there is intrinsic or acquired resistance to methotrexate on this basis (20–22).

Based upon immunohistochemical analyses, both the N- and C- termini of human and rodent PCFT are located within the cytoplasm consistent with an even number of transmembrane helices (10,23). The subsequent demonstration that two predicted N-linked glycosylation sites are, in fact, glycosylated in human PCFT, provided additional evidence for the extracellular location of the loop between the first and second TMDs (23). In the current paper, the substituted cysteine accessibility method (SCAM) was utilized to further characterize the membrane topology of PCFT (24). First, a functional cysteine-less PCFT (CL-PCFT) was generated, following which residues in predicted external and internal loops were replaced with cysteine, and the accessibility of the residues probed with a methanethiosulfonate-biotin reagent in the presence or absence of membrane permeabilization. The results provide evidence for a 12 TMD topology and an interaction between two native cysteine residues localized in extracellular loops.

Materials and Methods

Generation of PCFT mutant expression vectors by site-directed mutagenesis

The construction of a C-terminus HA- (haemagglutinin)-tagged human PCFT expression vector has been described (23). All PCFT mutants generated for this study were HA- tagged at the C-terminus. The CL-PCFT expression vector was generated in two steps with the QuikChange® Multi Site-Directed Mutagenesis Kit (Stratagene, La Jolla, CA). In the first step, C21, C66 and C151 were simultaneously replaced with serine and in the second step C229, C298, C328 and C397 were simultaneously changed to serine. The primers used in these procedures are listed in Table I. For introduction of cysteine residues into CL-PCFT, the QuikChange® II XL Site-Directed Mutagenesis Kit (Stratagene, La Jolla, CA) was utilized. The sense primers for these mutations are listed in Table I. For some mutations a temperature (50 °C) lower than the standard annealing temperature of 60 °C was required. The coding region of the final expression vectors was verified by automated sequencing in the Albert Einstein Cancer Center Genomics Shared Resource.

Cell lines and chemicals

HeLa cells were maintained in RPMI-1640 medium supplemented with 10% fetal bovine serum, 100 units/ml penicillin and 100 μg/ml streptomycin. [3′,5′,7-^{3}H(N)]-methotrexate was purchased from Moravek Biochemicals (Brea, CA). Other reagents utilized for SCAM are indicated below in the description of the specific methodologies.

Transport measurements

HeLa cells were seeded into 20mL Low Background glass scintillation vials (Research Products International Corporation, Prospect IL) at a density of 0.4 million cells/vial. The next day, cells were transfected with PCFT expression vectors (1 μg/vial) and Lipofectamine 2000

(2.5 μl/vial, Invitrogen, Carlsbad, CA) according to the manufacturer's protocol. [3H] methotrexate influx was assessed two days after transfection. Briefly, cells were washed twice with HBS (20mM HEPES, 5mM dextrose, 140mM NaCl, 5mM KCl, 2mM MgCl$_2$, pH 7.4) and incubated in the same buffer at 37°C for 20 min. The incubation buffer was then aspirated and transport was initiated by the addition of 0.5mL of pre-warmed (37 °C) MBS (20mM MES, 140mM NaCl, 5mM KCl, 2mM MgCl$_2$, pH 5.5) containing 0.5 μM [3H]methotrexate. Uptake was carried out at 37° over 2 min, which approximated initial rates under these conditions, and stopped by the addition of 5mL ice-cold HBS. Cells were washed three times with ice-cold HBS and dissolved in 0.5 mL of 0.2M NaOH at 65°C for 40 min. Radioactivity in 0.4mL of lysate was measured on a liquid scintillation spectrometer and normalized to protein levels obtained with the BCA Protein Assay (Pierce, Rockford, IL).

Biotinylation and immunoprecipitation

HeLa cells were seeded in 6 well plates at a density of 0.6 million cells per well. On day two, cells were transfected according to the manufacturer's protocol with HA-tagged PCFT expression vectors (2 μg/well) and Lipofectamin 2000 (5 μl/well). The serum-free RPMI 1640 medium employed in transfection protocol was replaced with normal growth medium four hours later. On day 3, the growth medium was replaced with fresh medium. Biotinylation was conducted on the fourth day with MTSEA-biotin (Biotium, Hayward, CA). MTSEA-biotin was dissolved in DMSO at a concentration of 2 mg/100 μl and then diluted with PBS at a ratio of 1 to 100. Cells that had been washed twice with 2 ml PBS were immediately incubated with this MTSEA-biotin solution (1ml/well) for 30 min at room temperature. The MTSEA-biotin solution was aspirated and the cells were washed twice with 2 ml PBS then overlaid on ice with 0.7 ml hypotonic buffer; (0.5 mM Na$_2$HPO$_4$, 0.1 mM EDTA, pH 7.0) containing protease inhibitor cocktail (Roche, Indianapolis, IN). The cells were then detached from the plates with disposable cell lifters and centrifuged at 16,000 X g and 4 °C for 5 min. The pellet was then resuspended in 0.4 ml lysis buffer (50 mM TRIS-base, 150 mM NaCl, 1% NP40, 0.5% sodium deoxycholate, pH 7.4) and mixed on a rotisserie shaker for 1 h at 4° before re-centrifugation at 16,000 X g and 4°C for 15 min. The supernatant was collected and identified as "crude membrane fraction"; 25 μL of this fraction was separated and stored at −20 °C. The remaining crude membrane fraction (~375 μL) was mixed on a rotisserie shaker overnight at 4°C with 50 μL of streptavidin agarose resin (Thermo Scientific, Rockford, IL) that was pre-washed three times with the lysis buffer. The next day (day 5), the mixture was centrifuged for 30 sec at 16,000 X g following which the supernatant was aspirated from the resin which was then washed 3 times with the 0.5 ml lysis buffer, each with a 20 min mix on a rotisserie shaker. The final wash was with the lysis buffer supplemented with 2% SDS. The precipitated proteins were released from the resin by heating at 95 °C for 5 min in 2X SDS-PAGE sample loading buffer containing dithiothreitol (DTT).

To optimize permeabilization, cells were initially incubated with different concentrations of digitonin in PBS for 5 min (25). A concentration of digitonin of 50 μg/ml was the minimum level required to permeabilize ~75% of HeLa cells (assayed by trypan blue exclusion) and was used in all studies. While a higher concentration of digitonin achieved greater permeabilization, this resulted in increased non-specific binding of proteins to the streptavidin agarose resin. To block cysteine residues with MTSES (Toronto Research Chemicals Inc, Canada), a concentration of 1 mg/ml of this reagent in PBS was prepared and immediately added (1ml/well) to pre-washed cells and incubated at room temperature for 30 min. To disrupt the disulfide-bridge, cells expressing WT-PCFT were treated with 20 mM β-mercaptoethanol in PBS for 30 min at room temperature followed by two washes with PBS.

Western blotting analysis

All samples were resolved on standard 12.5% SDS-PAGE without reducing reagent. The precipitated proteins (released from beads as described in see previous sections) were loaded directly on gels while the crude membranes were mixed (1:1) with DTT-containing 2X SDS-PAGE sample loading buffer at room temperature before loading on gels. After SDS-PAGE, proteins were transferred to Amersham Hybond membranes (GE Healthcare, Piscataway, NJ). The membranes were blocked with 10% dry milk in TBST (20 mM Tris, 135 mM NaCl, 1% Tween 20, pH 7.6) overnight and probed for 2 hr with a rabbit anti-HA antibody (#H6908, Sigma, St Louis, MI) at a dilution of 1:5000 in TBST containing 0.1 % dry milk. After 3 washes with TBST, membranes were incubated for 1 hr on a shaker with anti-rabbit IgG-HRP conjugate (Cell Signaling Technology) in TBST at a 1:5000 dilution. After three additional washes with TBST, the blots were developed with Amersham ECL Plus reagent (GE Healthcare, Piscataway, NJ) and exposed to autoradiography film (Denville Scientific, Metuchen, NJ).

Results

A working model of human PCFT membrane topology

Different computer programs used by different servers predict a different number of transmenbrane domains (TMDs) for human PCFT topology. For example, 12-, 11, or 10-TMD models are predicted by HMMTOP (26), TMHMM (27) or TMpred (28), respectively. Based upon the findings that both C- and N-termini are localized intracellularly and both predicted N-glycosylation sites (N58 and N68) are actually glycosylated, an even number of TMDs was required and a 12-TMD-topology wa utilized as a working model for the current study (Fig. 1).

Generation of cysteineless human PCFT

There are seven cysteine residues in human PFCT (Fig. 1); their exact positions are indicated in Table I. All these residues were replaced with serine to generate a cysteine-less PCFT or CL-PCFT. As indicated in Fig. 2, [3H]methotrexate influx mediated by CL-PCFT was ~85% that of WT-PCFT, a difference that did not reach statistical significance based upon the average of six independent experiments.

Introduction of cysteine residues in loops predicted to be extracellular or intracellular in the CL-PCFT

Since the locations of the N- and C-termini as well as the first predicted extracellular loop (EL1) are established, the current study focused on predicted extracellular loops, EL 2 to EL 6, and predicted intracellular loops (IL), IL 1 to IL 5 (Fig. 1). One residue in each targeted loop, except IL3, was mutated to cysteine. Two residues in IL3 were individually mutated to cysteine due to the large size of this loop (Fig. 1 and Table 1). The resulting mutants met two basic requirements of SCAM. (i) The mutated PCFT retained function. (ii) The mutated PCFT could be labeled either in the absence or presence of membrane permealization.

Transport function for each PCFT mutant was assessed. As indicated in Fig. 3, the majority of the mutant PCFTs had [3H]methotrexate influx activities similar to, or slightly less than, that of CL-PCFT. Activity of the L357C mutant was 38% of CL-PCFT; this was far higher than that of the mock-transfected cells.

Biotinylation of PCFT mutants with MTSEA-biotin in the absence of permeabilization

Biotinylation of PCFT mutants was carried out with a membrane-impermeant reagent, MTSEA-biotin, in the absence of permeabilization. Under these conditions, only externally

accessible cysteine residues can be labeled. As indicated in Fig. 4, Panel A, upper bands, V141C (EL 2), G207C (EL 3), E292C (EL 4), L357C (EL 5) and T417C (EL 6) mutants were labeled by MTSEA-biotin. CL-PCFT was not labeled as expected. It is interesting to note that WT-PCFT was also not labeled, despite the presence of two (C66, EL1; C298, EL4) extracellular cysteine residues (Fig. 1). As a control, the amount of PCFT protein in the crude membrane preparation was also monitored (Panel A, lower bands). Consistent with the lower transport activity, L357C protein in the crude membrane preparation was less than that of CL-PCFT. For all mutants as well as WT-PCFT, protein migrates as a broad band on SDS-PAGE between 60–80 kDa, consistent with N-glycosylation of this transporter (23).

If cysteine residues in V141C, G207C, E292C, L357C and T417C mutants are indeed externally accessible, they should react with a cysteine-specific membrane-impermeant reagent, MTSES, thereby blocking subsequent biotinylation of these residues by MTSEA-biotin. As indicated in Panel B of Fig. 4, pre-treatment of intact cells expressing these mutants with MTSES reduced, or near completely eliminated, their subsequent biotinylation. These results further confirm the extracellular accessibility of these residues. There was no signal at all observed for CL-PCFT, indicating that the labeling is highly specific.

Biotinylation of PCFT mutants with MTSEA-biotin after membrane permeabilization

The remaining mutants, that could not be labeled by MTSEA-biotin in the absence of permeabilization, were then treated with this reagent after cells were permeabilized with digitonin. As indicated in Panel A of Fig. 5, S110C (IL 1), S174C (IL 2), T240C (IL 3), E261C (IL 3), L329C (IL 4) and T386C (IL 5) were labeled under these conditions, consistent with the intracellular localization of these residues.

Panel B of Fig. 5 confirms the intracellular location of cysteine residues in S110C, S174C, T240C, E261C, L329C and T386 mutants. Condition "1" indicates standard biotinylation after permeabilization with digitonin, the same condition as described for Panel A of this figure. Under condition "2", the intact cells were first treated with MTSES, the membrane-impermeant, cysteine-specific reagent followed by permeabilization of cells with digitonin before biotinylation with MTSEA-biotin. Since MTSES does not diffuse into cells, intracellularly localized cysteine residues should not be blocked, and biotinylation should not be affected.

This was what was observed. Under condition "3", cells were first permeabilized with digitonin, than treated with MTSES followed by biotinylation with MTSEA-biotin. Under this condition, the cells were permeable to MTSES resulting in its reaction with intracellularly localized cysteine residues thereby blocking the subsequent biotinylation of the mutants.

Identification of an intramolecular disulfide bridge between native cysteine 66 and cysteine 298 residues in human PCFT

As indicated above, WT-PCFT was not labeled with MTSEA-biotin in the absence of membrane permealization despite the fact that two native cysteine residues, C66 and C298 were localized to EL 1 and EL 4, respectively. One explanation for this finding is that both cysteine residues were not accessible to labeling reagent due to steric hindrance. Another possibility is that these residues form a disulfide bridge and thus no sulfhydryl groups are available for the labeling reaction. The following studies were designed to test these possibilities.

First, cells expressing WT-PCFT were treated with β-mercaptoethanol to disrupt a potential disulfide bridge thereby releasing sulfhydryl groups. As indicated in Panel A of Fig. 6, pre-treatment of cells with β-mercaptoethanol resulted in labeling of WT-PCFT with MTSEA-

biotin in the absence of permealization. Next, C66, C298, or both residues in WT-PCFT were substituted with serine to generate C66S, C298S, and C66S/C298S mutants. As expected, the activities of C66S, C298S or C66S/C298S, assessed by [³H]methotrexate influx, were comparable to that of WT-PCFT (95±5 %, 90±1 % or 96±5 % of WT-PCFT activity, respectively, based upon three independent experiments). As indicated in Panel B of Fig. 6, replacement of either C66 or C298 with serine allowed PCFT to be labeled by MTSEA-Biotin indicating that elimination of one cysteine of the disulfide bridge frees the other cysteine for the reaction. When both cysteine residues were removed from WT-PCFT, the mutant was not labeled by the MTSEA-biotin. Hence, these data are consistent with the presence of a disulfide bond between the C66 and C298 residues. It is of interest that PCFT protein migrates on SDS-PAGE as distinct double bands (Fig. 6) in the absence of the disulfide bond as compared a single band in the presence of the disulfide bond (Fig. 4 and 5).

Additional studies were designed to determine whether the disulfide bridge is intra- or inter-molecular; in the latter case the bond would represent the formation of a dimer or polymer among two or more PCFT molecules. If the disulfide bond was formed intermolecularly, the molecular size of PCFT would be twice that of the monomer or higher and would migrate much slower on SDS-PAGE in the absence any reducing reagent. WT-PCFT, C66S, C298C as well as C66S/C298S mutants were thus treated with the SDS-PAGE sample buffer in the absence of DTT along with a control where the treatment was performed in the presence of DTT to disrupt the disulfide bond. No change in migration was seen on SDS-PAGE under these two conditions for WT-PCFT, indicating the absence of an intermolecular disulfide bond in WT-PCFT (data not shown). In addition, the migration pattern for C66S, C298S and C66/C298 mutants was the same as WT-PCFT, regardless of the presence of DTT. Hence, the disulfide bridge formed between C66 and C298 is intramolecular.

Discussion

The current study utilized SCAM to define the localization of loops connecting PCFT transmembrane domains, an approach that has been applied to thoroughly characterize structural aspects of the reduced folate carrier (SLC19A1), the other major facilitative folate transport carrier (29–31). These data along with earlier immunohistochemical localization of the N- and C- termini of the human and murine PCFT within the cytoplasm indicate a PCFT topology consisting of twelve transmembrane domains. This is different than an earlier model of this carrier suggesting nine TMDs with the C-terminus localized extracellularly (32). Of course, ultimate resolution of the topology and three dimensional structure of PCFT will require a high-resolution crystal structure which has not as yet been achieved for a eukaryotic transporter.

The localization of two cysteine mutants (T240C and E261C), inserted near the membrane-aqueous boundaries of the large central loop (IL3), to the intracellular compartment confirms the location of the fully conserved H247 residue. Likewise, the results with the S174C mutant confirm the location of the fully conserved S172 at IL2. Homology modeling predicted, and site-directed mutagenesis supported, the likelihood that these residues are in hydrogen bond distance and influence the accessibility of folate substrates to the binding pocket within the translocation pathway (9). The integrity of the association between these two residues was also shown to limit proton slippage through the PCFT aqueous translocation pathway independent of folate substrate transport (9). Likewise, the data confirm the location of H281 in the 7ᵗʰ TMD, a residue that appears to influence proton binding which, in turn, modulates folate binding (9). The E185 residue, which plays an important role in proton-coupling, is confirmed to reside as predicted, in the 5ᵗʰ TMD (33). Confirmation of the secondary structure also strengthens localization of other PCFT residues mutated in patients with HFM (2,5).

The observation that two native cysteine residues, C66 and C298, in WT-PCFT could not be labeled by MTSEA-biotin in spite of their extracellular location led to identification of an intramolecular disulfide bridge between these two residues. Apparently, the formation of this disulfide bond is not critical to PCFT function since the C66S, C289S, C66S/C298S mutants and even CL-PCFT have transport activities comparable to that of WT- PCFT. This is in contrast to the more important role disulfide bridges play in other transporters. For example, the intramolecular bridge between C592 and C608 in the multidrug resistance-associated protein, ABCG2, is critical for membrane targeting and function (34). The disulfide bridge between C180 and C329 in the human proton-coupled amino acid transporter, hPAT1, is required for substrate binding (35). Disruption of the disulfide bond between C126 and C333 in the human vesicle monoamine transporter (VMAT2) impairs transport function (36). Elimination of the bridge between C255 and C511 in the human sodium/glucose cotransporter (SGT1) alters conformation of the transporter and decreases its affinity for α-methyl-glucose (37). All cysteine-associated disulfides bridges, as described above, are located extracellularly.

In the absence of a crystal structure, homology models have been employed to characterize eukaryotic facilitative transporters based upon the known structures of bacterial transporters (38). In the case of human PCFT, its structure has been predicted using the template of the bacterial glycerol-3-phosphate transporter- GlpT (5,9). The results from the current study not only verify the 12-transmembrane-domain-topology of human PCFT, but also provide new structural information that will allow refinement of the homology model. Hence, the substituted residues in the extracellular and intracellular loop must be exposed to their respective aqueous compartments since they are fully accessible to the MTSEA-biotin. Further, the native cysteine 66 in EL 1 must be physically close to cysteine 298 in EL4 within the context of the tertiary structure since these two residues form a disulfide bridge.

Other approaches to determine transporter topology utilize insertion of an immunoreactive epitope or N-glycosylation site. For example, along with SCAM (29), insertion of haemagglutinin (HA) (39,40) and N-glycosylation (40) sites have been used to determine the topology of human reduced folate carrier. Major advantages of SCAM include minimal structural effects associated with cysteine substitutions as well as rapid and selective reaction of the cysteine sulfhydryl group. Epitope insertion requires introduction of multiple sequential amino acid residues in a transporter, an alteration likely to affect transport function. Also, an antibody is much more likely to be inaccessible to the epitope then the much smaller sulfhydryl reagents. For N-glycosylation scanning mutagenesis, a predicted N-glycosylation site (NXS/T) may not be glycosylated, even if it is extracellularly located, if the targeted loop is small. Also, this approach cannot be used for localization of intracellular loops.

Acknowledgments

Abbreviations

CL	cysteineless
EL	extracellular loop
IL	intracellular loop
TMD	transmembrane domain
MTSEA-biotin	(2-((biotinoyl)amino)ethyl methanethiosulfonate
MTSES	2-sulfonatoethyl methanethiosulfonate

| DTT	dithiothreitol
PCFT	the proton-coupled folate transporter
SCAM	substituted cysteine accessibility method
HFM	hereditary folate malabsorption

References

1. Qiu A, Jansen M, Sakaris A, Min SH, Chattopadhyay S, Tsai E, Sandoval C, Zhao R, Akabas MH, Goldman ID. Identification of an intestinal folate transporter and the molecular basis for hereditary folate malabsorption. Cell 2006;127:917–928. [PubMed: 17129779]

2. Zhao R, Min SH, Qiu A, Sakaris A, Goldberg GL, Sandoval C, Malatack JJ, Rosenblatt DS, Goldman ID. The spectrum of mutations in the PCFT gene, coding for an intestinal folate transporter, that are the basis for hereditary folate malabsorption. Blood 2007;110:1147–1152. [PubMed: 17446347]

3. Min SH, OHSY, Karp GI, Poncz M, Zhao R, Goldman ID. The clinical course and genetic defect in the PCFT in a 27-year-old woman with Hereditary folate malabsorption. J Pediatr 2008;153:435–437. [PubMed: 18718264]

4. Meyer E, Kurian MA, Pasha S, Trembath RC, Cole T, Maher ER. A novel PCFT gene mutation (p.Cys66LeufsX99) causing hereditary folate malabsorption. Mol Genet Metab. 2009 Epub ahead of print.

5. Lasry I, Berman B, Straussberg R, Sofer Y, Bessler H, Sharkia M, Glaser F, Jansen G, Drori S, Assaraf YG. A novel loss of function mutation in the proton-coupled folate transporter from a patient with hereditary folate malabsorption reveals that Arg 113 is crucial for function. Blood 2008;112:2055–2061. [PubMed: 18559978]

6. Borzutzky A, Crompton B, Bergmann AK, Giliani S, Baxi S, Martin M, Neufeld EJ, Notarangelo LD. Reversible severe combined immunodeficiency phenotype secondary to a mutation of the proton-coupled folate transporter. Clin Immunol 2009;133:287–294. [PubMed: 19740703]

7. Geller J, Kronn D, Jayabose S, Sandoval C. Hereditary folate malabsorption: family report and review of the literature. Medicine (Baltimore) 2002;81:51–68. [PubMed: 11807405]

8. Zhao R, Matherly LH, Goldman ID. Membrane transporters and folate homeostasis: intestinal absorption and transport into systemic compartments and tissues. Expert Rev Mol Med 2009;11:e4. [PubMed: 19173758]

9. Unal ES, Zhao R, Chang MH, Fiser A, Romero MF, Goldman ID. The functional roles of the His247 and His281 residues in folate and proton translocation mediated by the human proton-coupled folate transporter SLC46A1. J Biol Chem 2009;284:17846–17857. [PubMed: 19389703]

10. Qiu A, Min SH, Jansen M, Malhotra U, Tsai E, Cabelof DC, Matherly LH, Zhao R, Akabas MH, Goldman ID. Rodent intestinal folate transporters (SLC46A1): secondary structure, functional properties, and response to dietary folate restriction. Am J Physiol Cell Physiol 2007;293:C1669–C1678. [PubMed: 17898134]

11. Zhao R, Qiu A, Tsai E, Jansen M, Akabas MH, Goldman ID. The proton-coupled folate transporter (PCFT): impact on pemetrexed transport and on antifolate activities as compared to the reduced folate carrier. Mol Pharmacol 2008;74:854–862. [PubMed: 18524888]

12. Umapathy NS, Gnana-Prakasam JP, Martin PM, Mysona B, Dun Y, Smith SB, Ganapathy V, Prasad PD. Cloning and functional characterization of the proton-coupled electrogenic folate transporter and analysis of its expression in retinal cell types. Invest Ophthalmol Vis Sci 2007;48:5299–5305. [PubMed: 17962486]

13. Cronstein BN. Low-dose methotrexate: a mainstay in the treatment of rheumatoid arthritis. Pharmacol Rev 2005;57:163–172. [PubMed: 15914465]

14. Yokooji T, Mori N, Murakami T. Site-specific contribution of proton-coupled folate transporter/haem carrier protein 1 in the intestinal absorption of methotrexate in rats. J Pharm Pharmacol 2009;61:911–918. [PubMed: 19589233]

15. Chattopadhyay S, Moran RG, Goldman ID. Pemetrexed: biochemical and cellular pharmacology, mechanisms, and clinical applications. Mol Cancer Ther 2007;6:404–417. [PubMed: 17308042]

16. Vogelzang NJ, Rusthoven JJ, Symanowski J, Denham C, Kaukel E, Ruffie P, Gatzemeier U, Boyer M, Emri S, Manegold C, Niyikiza C, Paoletti P. Phase III Study of Pemetrexed in Combination With Cisplatin Versus Cisplatin Alone in Patients With Malignant Pleural Mesothelioma. J Clin Oncol 2003;21:2636–2644. [PubMed: 12860938]

17. Hanna N, Shepherd FA, Fossella FV, Pereira JR, De Marinis F, Von Pawel J, Gatzemeier U, Tsao TC, Pless M, Muller T, Lim HL, Desch C, Szondy K, Gervais R, Shaharyar, Manegold C, Paul S, Paoletti P, Einhorn L, Bunn PA Jr. Randomized Phase III Trial of Pemetrexed Versus Docetaxel in Patients With Non-Small-Cell Lung Cancer Previously Treated With Chemotherapy. J Clin Oncol 2004;22:1589–1597. [PubMed: 15117980]

18. Scagliotti GV, Parikh P, Von Pawel J, Biesma B, Vansteenkiste J, Manegold C, Serwatowski P, Gatzemeier U, Digumarti R, Zukin M, Lee JS, Mellemgaard A, Park K, Patil S, Rolski J, Goksel T, De Marinis F, Simms L, Sugarman KP, Gandara D. Phase III study comparing cisplatin plus gemcitabine with cisplatin plus pemetrexed in chemotherapy-naive patients with advanced-stage non-small-cell lung cancer. J Clin Oncol 2008;26:3543–3551. [PubMed: 18506025]

19. Ciuleanu T, Brodowicz T, Zielinski C, Kim JH, Krzakowski M, Laack E, Wu YL, Bover I, Begbie S, Tzekova V, Cucevic B, Pereira JR, Yang SH, Madhavan J, Sugarman KP, Peterson P, John WJ, Krejcy K, Belani CP. Maintenance pemetrexed plus best supportive care versus placebo plus best supportive care for non-small-cell lung cancer: a randomised, double-blind, phase 3 study. Lancet 2009;374:1432–1440. [PubMed: 19767093]

20. Zhao R, Goldman ID. Resistance to antifolates. Oncogene 2003;22:7431–7457. [PubMed: 14576850]

21. Chattopadhyay S, Zhao R, Krupenko SA, Krupenko N, Goldman ID. The inverse relationship between reduced folate carrier function and pemetrexed activity in a human colon cancer cell line. Mol Cancer Ther 2006;5:438–449. [PubMed: 16505119]

22. Zhao R, Hanscom M, Chattopadhyay S, Goldman ID. Selective preservation of pemetrexed pharmacological activity in HeLa cells lacking the reduced folate carrier; association with the presence of a secondary transport pathway. Cancer Res 2004;64:3313–3319. [PubMed: 15126375]

23. Unal ES, Zhao R, Qiu A, Goldman ID. N-linked glycosylation and its impact on the electrophoretic mobility and function of the human proton-coupled folate transporter (HsPCFT). Biochim Biophys Acta 2008;1178:1407–1414. [PubMed: 18405659]

24. Karlin A, Akabas MH. Substituted-cysteine accessibility method. Methods Enzymol 1998;293:123–45. 123–145. [PubMed: 9711606]

25. Chen JG, Liu-Chen S, Rudnick G. Determination of external loop topology in the serotonin transporter by site-directed chemical labeling. J Biol Chem 1998;273:12675–12681. [PubMed: 9575231]

26. Tusnady GE, Simon I. Principles governing amino acid composition of integral membrane proteins: application to topology prediction. J Mol Biol 1998;283:489–506. [PubMed: 9769220]

27. Krogh A, Larsson B, von Heijne G, Sonnhammer EL. Predicting transmembrane protein topology with a hidden Markov model: application to complete genomes. J Mol Biol 2001;305:567–580. [PubMed: 11152613]

28. Hofmann K, Stoffel W. TMbase - A database of membrane spanning proteins segments. Biol Chem Hoppe Seyler 1993;374:166.

29. Cao W, Matherly LH. Analysis of the membrane topology for transmembrane domains 7–12 of the human reduced folate carrier by scanning cysteine accessibility methods. Biochem J 2004;378:201–206. [PubMed: 14602046]

30. Hou Z, Ye J, Haska CL, Matherly LH. Transmembrane domains 4, 5, 7, 8, and 10 of the human reduced folate carrier are important structural or functional components of the transmembrane channel for folate substrates. J Biol Chem 2006;281:33588–33596. [PubMed: 16923800]

31. Hou Z, Stapels SE, Haska CL, Matherly LH. Localization of a substrate binding domain of the human reduced folate carrier to transmembrane domain 11 by radioaffinity labeling and cysteine-substituted accessibility methods. J Biol Chem 2005;280:36206–36213. [PubMed: 16115875]

32. Shayeghi M, Latunde-Dada GO, Oakhill JS, Laftah AH, Takeuchi K, Halliday N, Khan Y, Warley A, McCann FE, Hider RC, Frazer DM, Anderson GJ, Vulpe CD, Simpson RJ, McKie AT. Identification of an intestinal heme transporter. Cell 2005;122:789–801. [PubMed: 16143108]

33. Unal ES, Zhao R, Goldman ID. Role of the glutamate 185 residue in proton translocation mediated by the proton-coupled folate transporter SLC46A1. Am J Physiol Cell Physiol 2009;297:C66–C74. [PubMed: 19403800]

34. Henriksen U, Fog JU, Litman T, Gether U. Identification of intra- and intermolecular disulfide bridges in the multidrug resistance transporter ABCG2. J Biol Chem 2005;280:36926–36934. [PubMed: 16107343]

35. Dorn M, Weiwad M, Markwardt F, Laug L, Rudolph R, Brandsch M, Bosse-Doenecke E. Identification of a disulfide bridge essential for transport function of the human proton-coupled amino acid transporter hPAT1. J Biol Chem 2009;284:22123–22132. [PubMed: 19549785]

36. Thiriot DS, Sievert MK, Ruoho AE. Identification of human vesicle monoamine transporter (VMAT2) lumenal cysteines that form an intramolecular disulfide bond. Biochemistry 2002;41:6346–6353. [PubMed: 12009896]

37. Gagnon DG, Bissonnette P, Lapointe JY. Identification of a disulfide bridge linking the fourth and the seventh extracellular loops of the Na+/glucose cotransporter. J Gen Physiol 2006;127:145–158. [PubMed: 16446504]

38. Lemieux MJ. Eukaryotic major facilitator superfamily transporter modeling based on the prokaryotic GlpT crystal structure. Mol Membr Biol 2007;24:333–341. [PubMed: 17710637]

39. Ferguson PL, Flintoff WF. Topological and functional analysis of the human reduced folate carrier by hemagglutinin epitope insertion. J Biol Chem 1999;274:16269–16278. [PubMed: 10347183]

40. Liu X, Matherly L. Analysis of membrane topology of the human reduced folate carrier protein by hemagglutinin epitope insertion and scanning glycosylation insertion mutagenesis. Biochim Biophys Acta 2002;1564:333–342. For Toc graphic Use Only. [PubMed: 12175915]
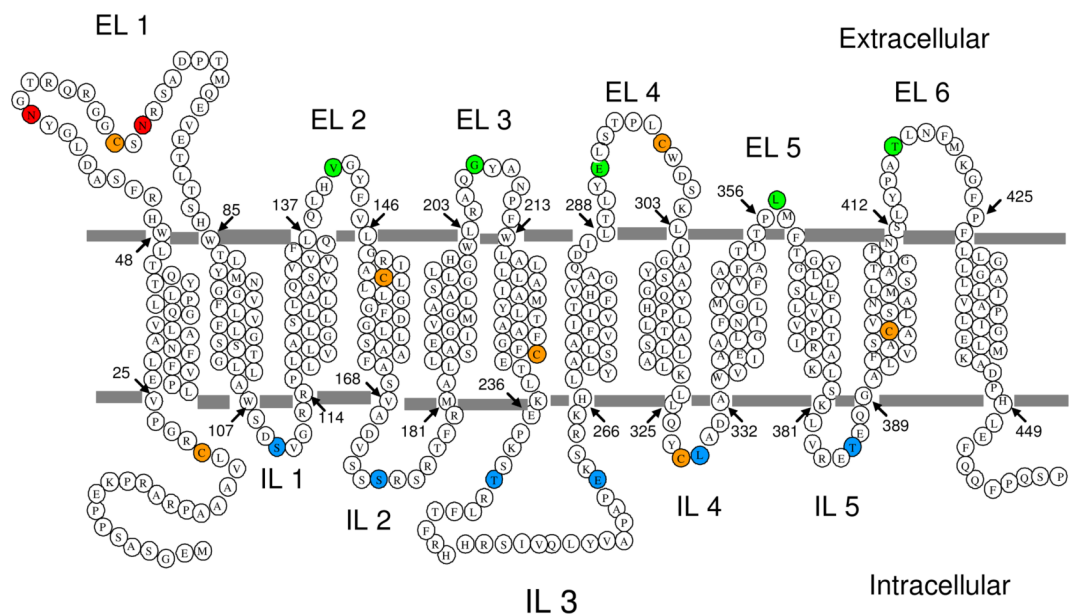
Figure 1. Membrane topology of human PCFT

A predicted model of the secondary structure of human PCFT (HMMTOP) supported by earlier reports (10,23) and the current study. Orange circles indicate seven native cysteine residues that were substituted with serine to obtain the cysteine-less protein, CL-PCFT. Green circles mark residues that could be biotinylated without membrane permealization while blues circles indicate residues that could be biotinylated only after membrane permeabilization. Red circles indicate sites of N-glycosylation. EL, extracellular loop; IL, intracellular loop.
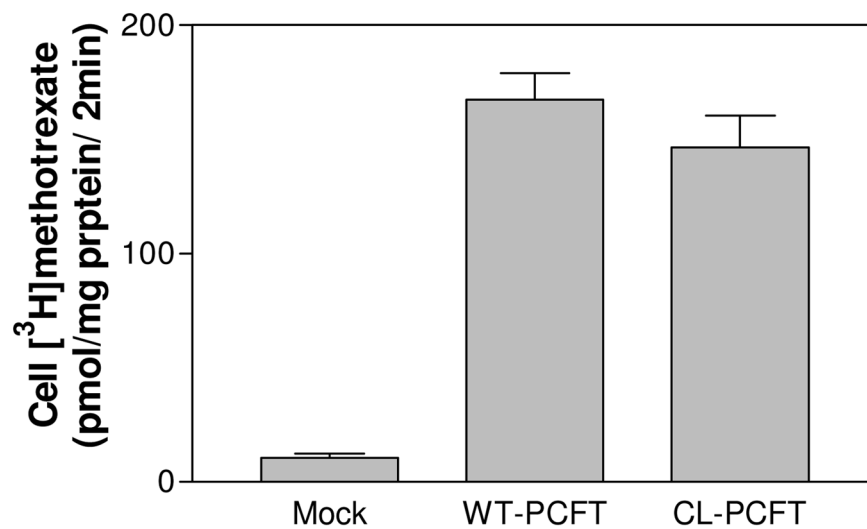
Figure 2. Assessment of CL-PCFT activity
CL-PCFT and WT-PCFT expression vectors were transiently transfected into HeLa cells. PCFT activity was determined 48 hr later by assessment of [³H]methotrexate influx (0.5 μM) at pH 5.5 over 2 min. Data are the mean ± SEM from 6 independent experiments.
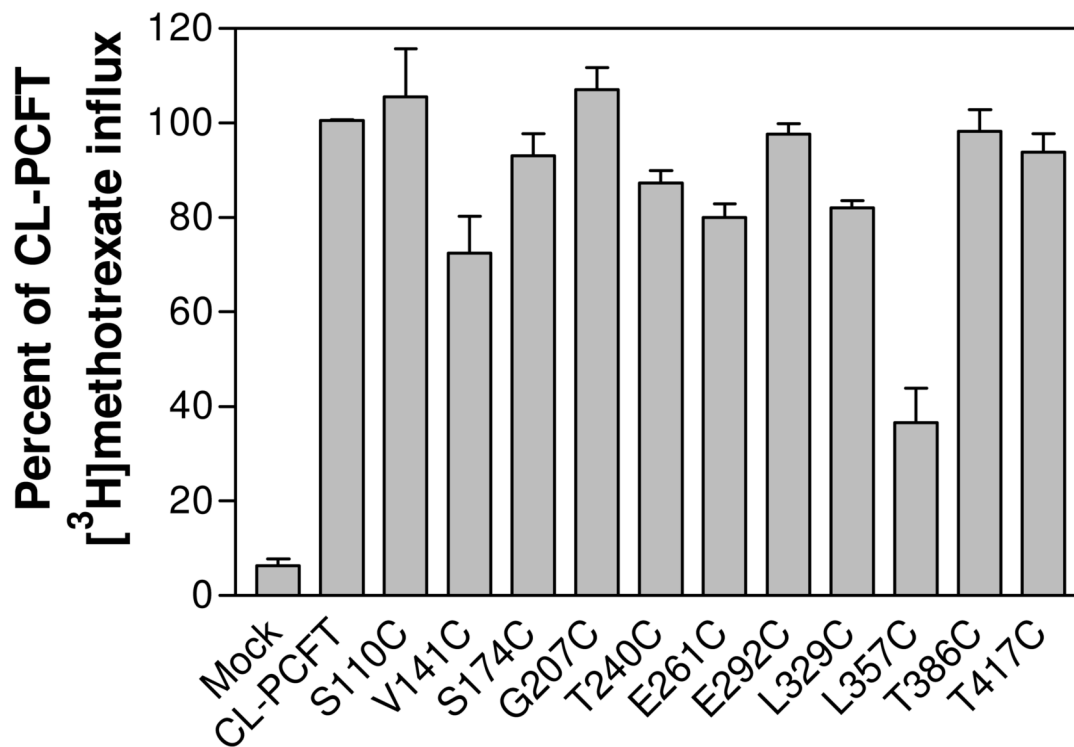
Figure 3. Assessment of transport activities of PCFT mutants generated for topological studies
CL-PCFT and mutant expression vectors were transiently transfected into HeLa cells. PCFT transport activities were assessed by 0.5 μM [^{3}H]methotrexate influx over 2 min at pH 5.5. The data for each mutant is expressed as percentage of CL-PCFT activity. The results are the mean ± SEM from three independent experiments.
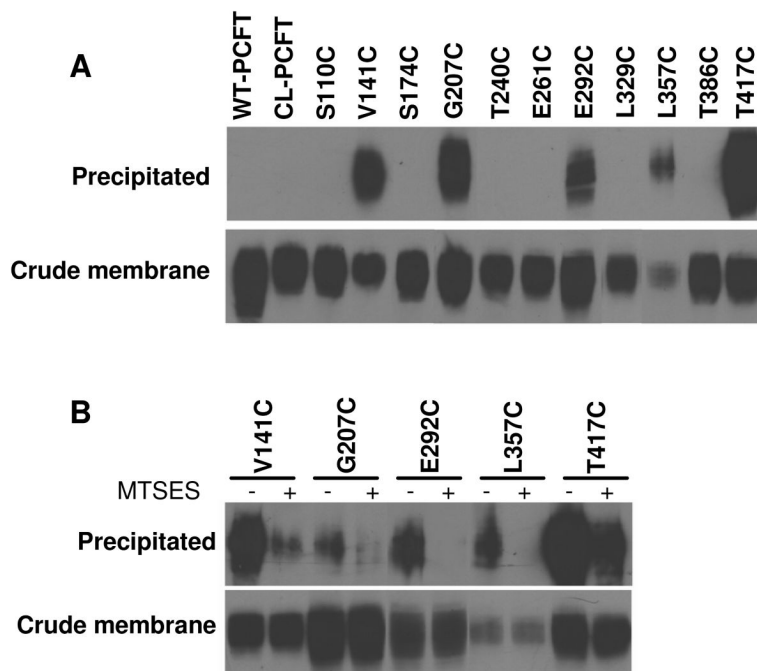
Figure 4. Bioinylation of PCFT mutants with MTSEA-biotin in the absence of permeabilization
HeLa cells transiently expressing HA-tagged WT-PCFT, CL-PCFT or PCFT mutants were treated with MTSEA-biotin and the crude membranes were then incubated with streptavidin beads to pull down biotinylated proteins. The proteins on the beads were recovered and analyzed by Western blot using an anti-HA antibody. PCFT protein in the crude membrane preparation was also analyzed to determine protein expression. **Panel A:** Representative labeling of PCFT expressed in HeLa cells with MTSEA-biotin in the absence membrane permealization (upper bands) along with total PCFT protein in crude membrane (lower panel). **Panel B:** Effect of pre-treatment with MTSES on biotinylation. The cells were either subjected directly to biotinylation or treated with MTSES before biotinylation. For both panels, at least two independent experiments were performed for each mutant and the crude membrane sample was always matched to the precipitated sample.
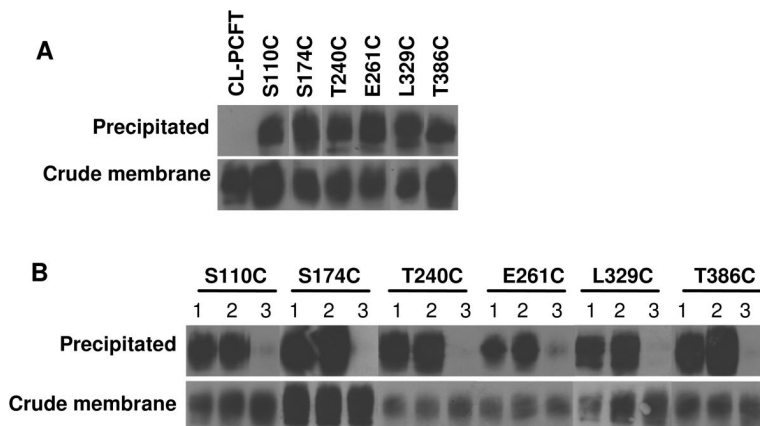
Figure 5. Bioinylation of PCFT mutants with MTSEA-biotin after permeabilization
Panel A: HeLa cells transiently expressing CL-PCFT or various mutants were permeabilized with digitonin before the biotinylation reaction. **Panel B: Dependence of biotinylation inhibition by MTSES on digitonin permeabilization.** Three conditions of biotinylation labeling were conducted for each mutant: (**1**) Cells were permeabilized before the biotinylation reaction (same as described for panel A of this figure). (**2**) Cells were first treated with MTSES, then permeabilized with digitinon before the biotinylation reaction. (**3**) Cells were permeabilized with digitonin first, then treated with MTSES before the biotinylation reaction. For all panels, the crude membrane sample was matched to the precipitated sample and results are representative of at least two separate experiments.
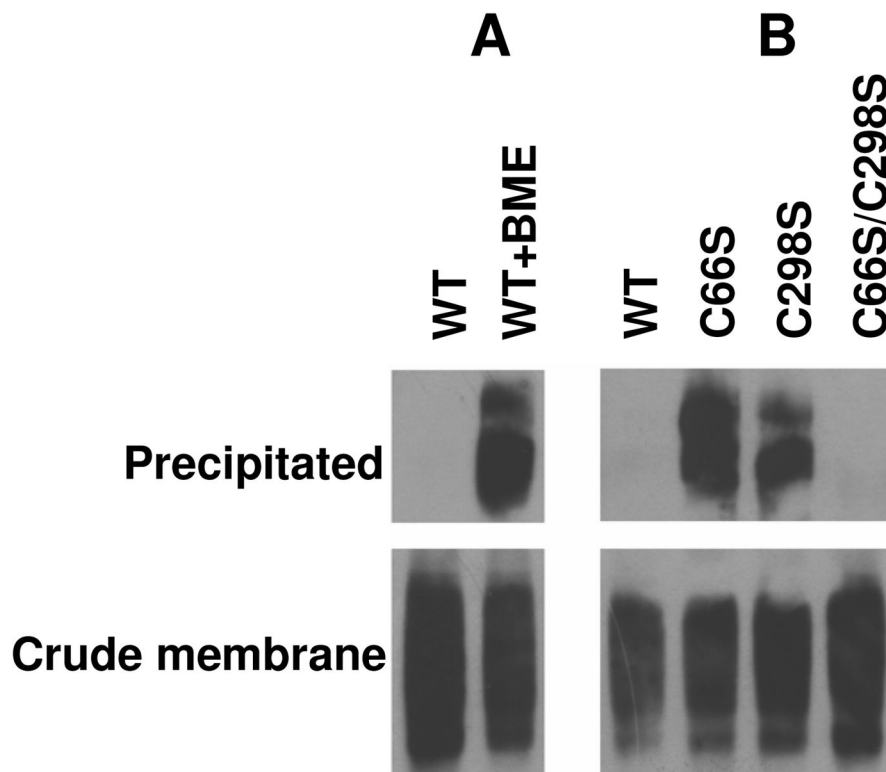
Fig. 6. Identification of a disulfide-bond between C66 and C298 in human PCFT
Panel A: The effect of treatment with 20 mM β-mercaptoethanol (BME) on biotinylation of HeLa cells expressing WT-PCFT. **Panel B:** Biotinylation of WT-PCFT and mutants in which C66, C298, or both was replaced with serine. For both panels, at least two independent experiments were performed for each mutant and the crude membrane sample was always matched to the precipitated sample.

Table I

Sense primers for generation of human PCFT mutants used in the current study

Mutations	Primer sequence (5′ to 3′)
C21S	GCGGCTGCCGTGCTGTCCCGGGGCCCGGTAGAG
C66S	CGCCAAAGGGGGGGGCTCCAGCAACCGCAGCGCG
C151S	CTGGGTCGCATCCTTTCTGCCCTCCTCGGCGAC
C229S	CTCTATGCAGCTTTCTCCTTTGGTGAGACCTTA
C298S	CTAAGCACACCCCTCTCCTGGGACTCCAAACTA
C328S	AAGCTCCTGCAGTACTCCCTGGCCGATGCCTGG
C397S	TTTTCTGCTGTGGCCTCTGTGAAATAGCCTGGCC
S110C	GGAGC TTGGAGCGAC TGTGTGGGCCGCCGCCCG
V141C	CAGCTGCAGCTCCACTGCGGCTACTTCGTGCTG
S174C	GATGTCAGCTCCTGCCGCAGCCGCACC
G207C	TGGCTCCGGGCCCAGTGTTATGCCAACCCCTTC
T240C	GAGCCAAAGTCCTGCCGGCTCTTCAC
E261C	GCTCCCGCCCCATGCAAGTCCAGGAAA
E292C	TTAACCCTTTATTGCCTAAGCACACCC
L329C	CTGCAGTACTCCTGCGCCGATGCCTGG
L357C	GCCACTATCACGCCTTGCATGTTCACAGGATAT
T386C	AAGCTGGTGAGAGAGTGCGAGCAGGGTGCTCTC
T417C	TCACTCTACCCAGCCTGTCTGAACTTTATGAAG